Colloid Polym Sci 278: 1085–1096 (2000)

ORIGINAL CONTRIBUTION

H.-D. Dörfler
A. Göpfert

Comparison of structures and properties of lyotropic cholesteric phases induced by center and axial chiral compounds

Received: 20 December 1999
Accepted: 22 May 2000

H.-D. Dörfler (✉) · A. Göpfert
TU Dresden, Institut für Physikalische Chemie und Elektrochemie, Kolloidchemie
Mommsenstr. 13,
D-01062 Dresden, Germany
Tel.: + +49 351 463 7638
Fax: + +39 351 463 7107

Abstract We studied the phase chirality in disklike lyotropic cholesteric (Ch_D) phases which were obtained by adding center and axial chiral dopants to achiral lyotropic nematic (N_D) host phases. In a lyotropic nematic matrix of the N_D phase in the hexadecyldimethylethylammonium bromide/water/*n*-decanol ternary system, a Ch_D phase was induced by adding center chiral sterols (cholesterol, prednisolon, taurocholic acid) and the axial optically active compound *R*(−)-1,1′-binaphthalene-2,2′-diyl-hydrogen phosphate (BDP). The helical twisting power (HTP) of BDP is generally lower than the HTP of inducing substances with center chirality, such as cholesterol, prednisolon, etc. At constant composition of the N_D phase, the helix lengths were determined from the ordered fingerprint texture, the so-called "spaghetti-like texture" seen in polarizing microscopy. The reciprocal helix lengths change linearly with the BDP concentration. The properties of the Ch_D phase (textures, helix lengths, micelle parameters) induced by the chiral compounds and changed by the composition of host phases give information on the mechanism of chirality transfer from the molecular level to that of the micellar aggregates and, eventually, to the liquid-crystalline superstructure. The structure in the Ch_D phase was described in the form of micelle parameters. For helix formation a minimum concentration of the chiral compounds is necessary. During the helix formation the number of micelles per helix length changes as a function of the concentration of the center and axial chiral molecules. The first step during the formation of the Ch_D phase is the solubilization of dopants into the micelles. Interaction between the optically active molecules then leads to the formation of hydrogen bridges between adjacent optically active molecules in the helical stack.

Key words Disklike lyotropic nematic phase · Disklike lyotropic cholesteric phase · X-ray diffraction scattering · Helix length · Center and axial chirality

Introduction

Chirality in liquid crystals, and in science generally, was the subject of many studies in the last 20 years. Lyotropic cholesteric phases were previously described [1–72]. Generally, the authors used a three-component system (water, surfactant, cosurfactant) to prepare the lyotropic nematic matrix. Optically active surfactants were applied to the formation of lyotropic cholesteric structures for the first time by Acimis and Reeves [39]. In their work they distinguished different types of lyotropic cholesteric phases. In the α-alanine hydrochloride decyl ester/water/Na_2SO_4 system a disklike cholesteric phase (Ch_D) was detected. The optical axis of this disk can be

oriented perpendicularly to the magnetic field. Radley and Saupe [40] were successful too in changing lyotropic nematic phases into lyotropic cholesteric ones by adding different optically active components (brucine sulfate, tartaric acid, cholesterol). Later [2–38] a lot of such multicomponent systems were investigated and described. The chemical natures of the substances in the ternary and quaternary systems were quite different. Also, optically active substances with different chemical structures were used.

In previous work [41–48] we studied the lyotropic nematic to lyotropic cholesteric transitions induced by selected chiral dopants. The addition of small amounts of chiral compounds, such as cholesterol, D- or L-tartaric acid, lithocholic acid, desoxycholic acid, cholic acid, Sodiumtaurocholate, hydrocortisone, prednisolone, etc., transformed lyotropic nematic phases into lyotropic cholesteric phases. The molecular mechanism by which twist is induced is not yet understood.

In the next step of our studies the pitch length was determined from the texture, oriented in a magnetic field, and the so-called helical twisting power (HTP) was evaluated. Four aspects were found to be important from our investigations and analysis of helix formation:

- Characterization of the lyotropic cholesteric phase using the axial chiral optically active compound *R*(−)-1,1′-binaphthalene-2,2′-diyl-hydrogen phosphate (BDP) by texture observations and using small- and wide-angle X-ray scattering (SWAXS). Analysis of the structural changes of the micelles in the Ch_D phase with respect to the BDP concentration.
- Analysis of the influence of the host phase – this means the influence of the composition in the lyotropic nematic matrix – on the properties of the lyotropic cholesteric phase by measurements of the pitch length and by SWAXS investigations.
- Comparison of the twisting properties of compounds with inherent dissymmetry, so-called center chiral optically active compounds with axial chiral optically active compounds.
- Analysis of the main factors for helix formation by evaluation of the scattering curves to obtain and compare structural parameters of the Ch_D phase induced by different optically active compounds (center chiral, axial chiral).

Experimental

Substances and sample preparation

Hexadecyldimethylethylammonium bromide p.a. ($C_{16}Me_2EABr$), *n*-decanol p.a. and prednisolone p.a. were products of Fluka (Switzerland). For purification this substance was subjected to twofold recrystallization from an ether/ethanol mixture. Cholesterol p.a. was from Merck (Darmstadt, Germany) and Sodiumtaurocholate p.a. was from Sigma-Aldrich Chemie (Deisenhofen, Germany). Both were used without further purification. The axial chiral optically active compound [R(−)-1, 1′-binaphthalene-2, 2′-diyl-hydrogen-phosphate = BDP] p.a. was a product from Sigma-Aldrich Chemie.

For the sample preparation, required amounts of each component (surfactant, cosurfactant, water, optically active substance) of the four-component system were weighed in 2-ml flasks and then homogenized by a powerful hot-air apparatus (type PHG 600 E, Bosch, Germany) and an intensive shaker (type VF2, Janke and Kunkel, Germany). The homogenized samples were kept at room temperature or at 300 K for 1–2 days. The samples were then used for texture observations and SWAXS measurements.

For texture observations and X-ray diffraction scattering, the samples were put into microslides (Camlab, UK) and oriented in the magnetic field of an electromagnet (Phylatex, Germany) with a magnetic field strength of 2.1 T. The same samples were used for polarizing microscopy and X-ray measurements. During the magnetic field alignment the samples were kept at constant temperature. Before the X-ray diffraction measurements the samples were equilibrated for about 45 min at the starting temperature. Samples were measured at each temperature for 30 min, and the equilibration time at each new temperature setting was 10 min.

Methods

Polarizing microscopy observation

To ensure correlation with the SWAXS measurements and for additional qualitative structural information, the samples were also checked by polarizing microscopy. A Jenapol 30-0060 stereoscopic microscope (Carl Zeiss Jena, Germany) equipped with an FP 82 microsample thermostat adapter and with an FP 80 control unit (both Mettler, Germany) were used. Effective texture identification of the lyotropic liquid crystals was supported by image recording during temperature ramping utilizing S-VHS video equipment (camera WV CL 70/G, recorder NV-FS 88 EG and monitor BT-HA 450 Y, all Panasonic, Japan). Optionally a Screen Machine video frame grabbler (Fast Electronics, Germany) was used to provide digital representations of images for further computational enhancements.

The pitch length, p, of the Ch_D phase was determined by polarizing microscopy (Fig. 1). For this purpose, we used a micrometer eyepiece with an engraved line micrometer. Our test object was a 0.2-mm thick sample aligned in the magnetic field which showed the ordered fingerprint texture (Fig. 2c). Under these conditions, the helical axis is parallel to the magnetic field (Fig. 1). The texture observed by polarization microscopy coincides with the vertical direction in the photograph and, in agreement with Fig. 1, it represents a section in the direction of the helical axis. p was determined with the aid of the micrometer of the microscope.

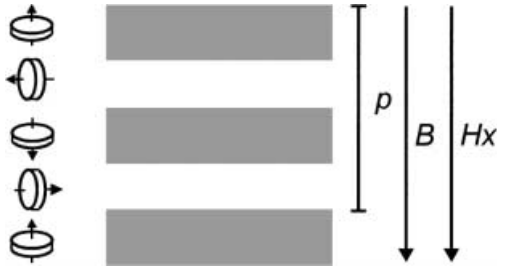

Fig. 1 Determination of the pitch length, p, with the aid of the "spaghetti-like texture" observed by polarizing microscopy. *B*, direction of the magnetic field; *Hx*, direction of the helix axis

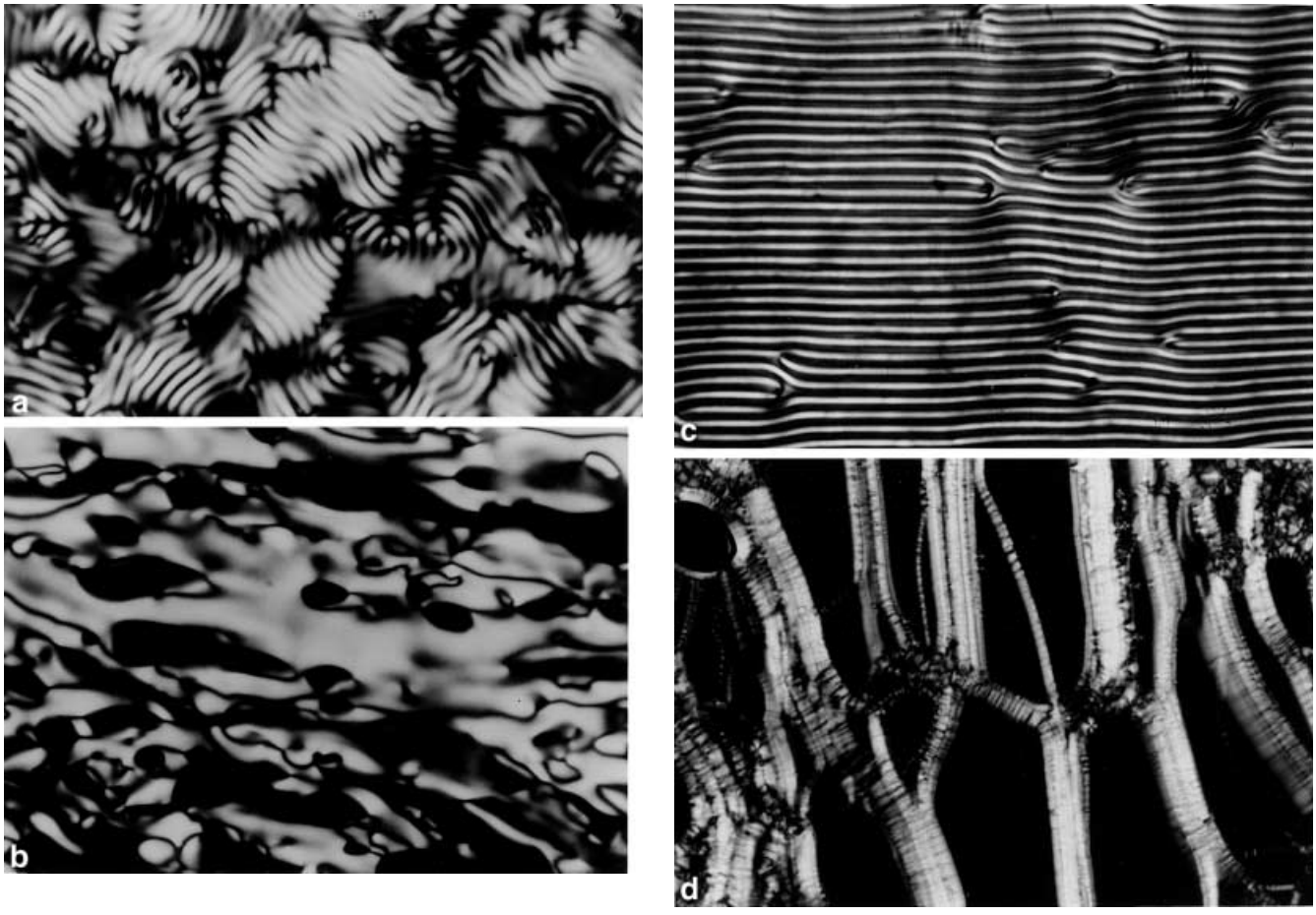

Fig. 2a–d Textures of different lyotropic liquid crystals at different temperatures in the Hexadecyldimethylethylammonium bromide ($C_{16}Me_2EABr$)/water/*n*-decanol/*R*(−)-1,1′-binaphthalene-2,2′-diyl-hydrogen phosphate (*BDP*) quaternary system. **a** "Fingerprint texture" of the nonaligned disklike lyotropic cholesteric (Ch_D) phase. **b** "Schlieren texture" of the nonaligned lyotropic nematic phase. **c** Ordered fingerprint texture, the so-called "spaghetti-like texture", of an oriented Ch_D phase. The Ch_D phase has been subjected to a magnetic field for 10 h (1.2 T). **d** "Oily streaks" of the lamellar L_α phase. Magnification 100×

Simultaneous Small and Wide-Angle X-ray Scaterring (SWAXS)

The measurements were carried out using a SWAXS camera (Hecus MBraun-Graz-X-ray Systems, Graz, Austria), with Kratky slit optics and two coupled linear position sensitive detectors (PSD, MBraun, Garching, Germany) for the small- and wide-angle ranges, respectively. The optical feature of the Kratky collimation system in combination with the PSDs for small-angle scattering and diffraction measurements were expanded to provide the possibilities for simultaneous small-angle (resolution range between 1000 and 10 Å with Cu radiation) and wide-angle measurements (in the range 3.4–4.9 Å). Scattering data from these two ranges were recorded by two PSDs and combined within one multichannel system.

The line focus (Cu K_α radiation) from an X-ray generator of the former Freiberger Präzisionsmechanik (Freiberg/Saxony, Germany) was used as a radiation source. The Cu K_β radiation was eliminated with a Ni filter. The detector position scaling was calibrated with characteristic reflexions of silver stearate (small-angle region at $d = 48.78$ Å) and *p*-bromobenzoic acid (wide-angle region at $d_1 = 4.67$ Å, $d_2 = 3.80$ Å and $d_3 = 3.70$ Å) as reference materials. All samples were contained in microslides as mentioned earlier, held in a steel cuvette to provide good thermal contact to the computer-controlled Peltier heating system (Hecus MBraun-Graz-X-ray Systems, Graz, Austria).

Results and discussion

Texture and helix lengths related to the BDP concentration

Helix formation took place in the $C_{16}Me_2EABr$/water/*n*-decanol/BDP four-component system. The "fingerprint texture" of the nonaligned Ch_D phase is shown in Fig. 2a. The Ch_D phase is partially oriented under the influence of the glass walls. During this orientation the polar head groups of the surfactants or cosurfactants point outward. Neighboring micellar aggregates also align so that their long axis is parallel to the interface. At a given distance, this reduces the electrostatic repulsion to the surface. In analogy to the lyotropic nematic phases the corresponding lyotropic cholesteric phase can also be aligned by a magnetic field.

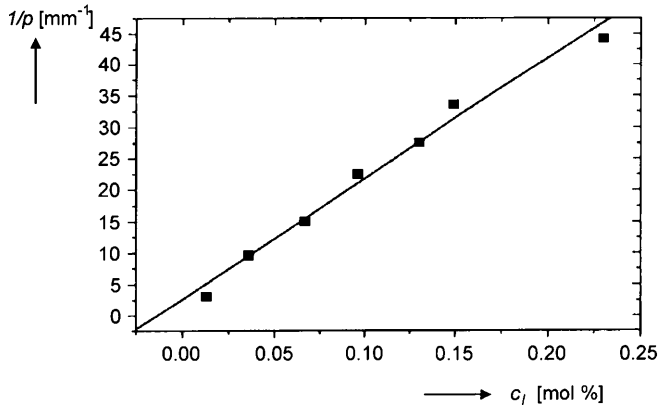

Fig. 3 Reciprocal pitch length, $1/p$, obtained by evaluating the "spaghetti-like" texture (Fig. 1) as a function of the BDP concentration, c_I, at 298 K. Composition of the Ch_D phase: 28 wt% $C_{16}Me_2EABr$; 67.7 wt% water; 4.3 wt% *n*-decanol; + BDP

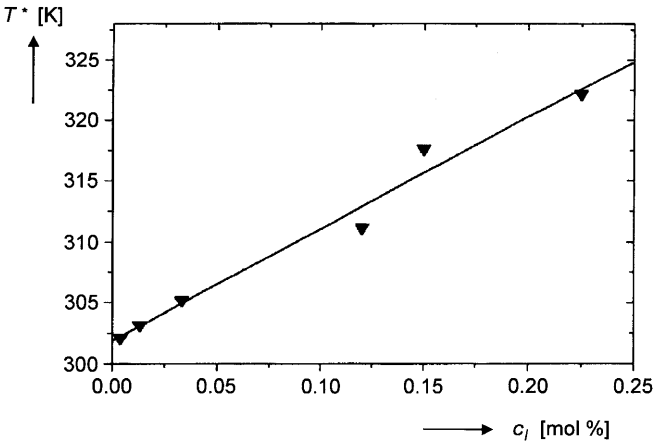

Fig. 4 Variation of the temperatures, T^*, of the $Ch_D \rightarrow S$ (isotropic phase) phase transition with the BDP concentration. Composition of the Ch_D phase: 28 wt% $C_{16}Me_2EABr$; 67.7 wt% water; 4.3 wt% *n*-decanol; + BDP

In the rodlike lyotropic cholesteric Ch_C phase the helical structure unwinds. The application of an external magnetic field leads to a nematic "Schlieren texture" (Fig. 2b). In the Ch_D phase, however, the formation of cholesteric structure can easily be observed by polarizing microscopy. Only one domain of the "fingerprint texture" shows ordered morphology (Fig. 2a). These domains can be aligned by an external magnetic field. Then, the typical "spaghetti-like texture" is observed (Fig. 2c).

A point of special interest in texture observations was the change in pitch length effected by BDP. The results are illustrated in Fig. 3. At low BDP concentrations the reciprocal pitch length increases linearly. Using Eq. (1) the HTP values of the optically active compound BDP at constant temperature were calculated:

$$(HTP)_T = \lim_{c_I \rightarrow 0} \frac{1}{pc_I} \quad , \tag{1}$$

with p the helix length, c_I the concentration of BDP and HTP = 192.3 mm^{-1} mol^{-1}. This indicates that the HTP value of BDP is very low in comparison to those of cholesterol, prednisolone, etc. The temperatures, T^*, of the $Ch_D \rightarrow S$ phase transition increase linearly with the BDP concentration (Fig. 4).

SWAXS measurements and influence of BDP on the structure formation in the Ch_D phase

Some small-angle X-ray diffraction patterns of the Ch_D phase for different BDP concentrations are collected in Fig. 5. An interesting feature of the SWAXS pattern is that under the condition of parallel X-raying, the positions of the (1 0 0) and (2 0 0) reflexes are not dependent on the BDP concentration. The same phenomenon was observed when cholesterol was added to induce the Ch_D phase [46]. Otherwise under the

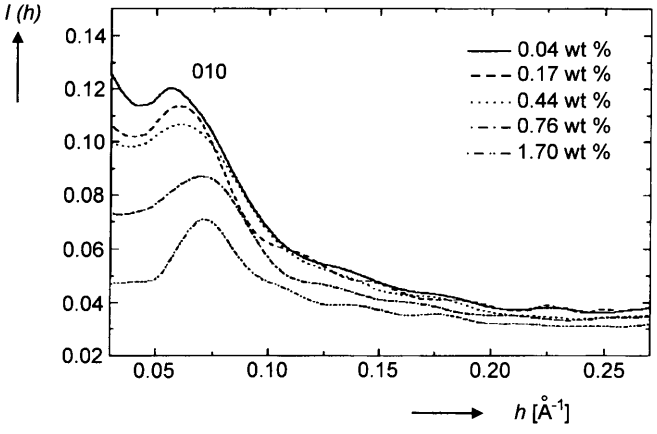

Fig. 5 Experimental scattering curve (desmeared) of the Ch_D phase under the conditions of the perpendicular X-raying of the sample as a function of the BDP concentration (c_I in wt%). Composition of the Ch_D phase: 28 wt% $C_{16}Me_2EABr$; 67.7 wt% water; 4.3 wt% *n*-decanol; + BDP. I (h), scattering intensity; h, scattering vector [$h = (4\pi/\lambda)\sin(\Theta/2)$; λ, wave length of the radiation; Θ scattering angle]

condition of perpendicular X-raying of the sample, the (0 1 0) reflex shifts with increasing BDP concentration to higher values. These results are summarized in Fig. 6.

The aim of the SWAXS measurement was to calculate some micelle parameters of the Ch_D phase using the X-ray diffraction curves shown in Fig. 5. The periodic volume, V_P, is given by

$$V_P = \frac{\pi}{4} d_s^2 \, d_p \quad , \tag{2}$$

with d_s the Bragg values under the conditions of perpendicular X-raying and d_p the Bragg values under the conditions of parallel X-raying. The volume of the micelles, V_M, can be simply expressed by

$$V_M = V_P(1 - \phi) \ , \qquad (3)$$

with ϕ the volume fraction of the samples. The theoretical background is described in Ref. [69]. To calculate the anisotropy of the periodic volume we measured the SWAXS patterns at different BDP concentrations (Fig. 7, Table 1). The analysis of the micelle parameters clearly proves the solubilization of the BDP molecules into the micelles. The solubilization is accompanied by a change in the micelle parameters (Table 1). The micelle volume rises considerably. We assume that the optically active compounds in the bilayer of the disklike micelles arrange between the surfactant and cosurfactant molecules in the position with the smallest curvature of the micelles. Thus, the distribution of the BDP molecules in the micelles is not homogeneous; therefore, each composition of the micelle interface will have its own local concentration profile which changes the curvature of the micelles. This situation is outlined in Fig. 8a in comparison to the solubilization of cholesterol into the micelles of the disklike lyotropic nematic (N_D) phase (Fig. 8b).

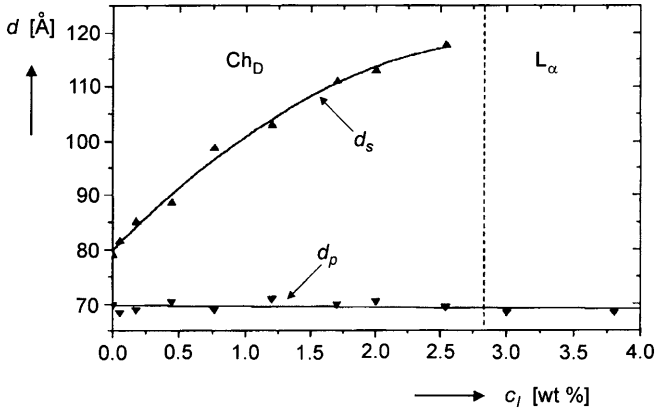

Fig. 6 Anisotropy ($A = d_s/d_p = d_{0\,1\,0}/d_{1\,0\,0}$) of the periodic volume as a function of the BDP concentration at 298 K under the conditions of the X-rays parallel (index p, ▼) and perpendicular (index s, ▲) to the sample. Composition of the Ch_D phase: 28 wt% $C_{16}Me_2EABr$; 67.7 wt% water; 4.3 wt% *n*-decanol. *d* is the Bragg value

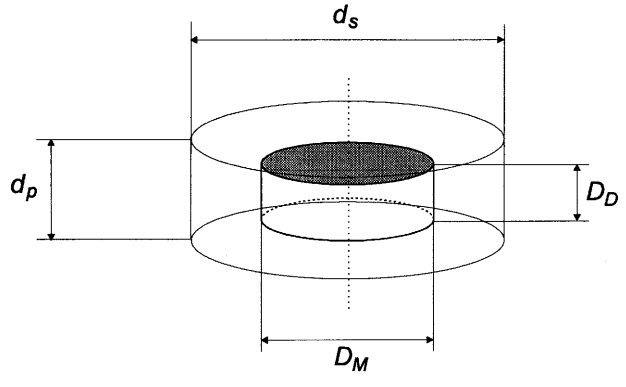

Fig. 7 Illustration of the periodic volume of a micellar unit, evaluated from the first maximum of the scattering curves. D_D, thickness of the micelle; D_M, diameter of the micelle; d_s, Bragg values under the conditions of perpendicular X-raying; d_p, Bragg values under the conditions of parallel X-raying

Table 1 Micelle parameters of the induced disklike lyotropic cholesteric Ch_D phase as function of the *R*(−)-1,1′-binaphthalene-2, 2′-diyl-hydrogen phosphate (*BDP*) concentration, c_I, at 298 K. Composition of the matrix of the disklike lyotropic nematic (N_D) phase: 28 wt% hexadecyldimethylethylammonium bromide ($C_{16}Me_2EABr$); 67.7 wt% water; 4.3 wt% *n*-decanol. V_P, periodic volume of the micelle; V_M, micelle volume; $d_{0\,1\,0}/d_{1\,0\,0} = d_s/d_p = A$, the anisotropy of the periodic volume; $\bar{z}_A$, average aggregation numbers per micelle; $\bar{z}_I$, average solubilization numbers of BDP molecules per micelle; $\bar{z}_M$, average micelle numbers per helix length

c_I (wt%)	V_P (10^5 Å^3)	V_M (10^5 Å^3)	$A = d_{0\,1\,0}/d_{1\,0\,0}$	$\bar{z}_A$	$\bar{z}_I$	$\bar{z}_M$
0	3.64	1.20	1.17	161	0	–
0.17	3.91	1.29	1.21	172	1	18800
0.44	4.35	1.43	1.27	192	3	6200
0.76	5.09	1.71	1.37	224	6	3800
1.7	6.53	2.26	1.54	284	17	1800
2.0	6.77	2.36	1.58	298	21	1330

Influence of the composition in the lyotropic nematic host phase on the properties of the lyotropic cholesteric phase

As mentioned previously alignment of the Ch_D phase in a magnetic field produced an ordered fingerprint texture at 298 K (Fig. 2c). A point of special interest in the texture observation was again the change in the pitch length when the composition of the matrix in the N_D phase was changed (Fig. 9).

T^* of the $N_D \rightarrow S$ and $Ch_D \rightarrow S$ transitions as a function of the surfactant concentration in the N_D phase and in the Ch_D phase are shown in Fig. 10. At high surfactant concentrations T^* increases linearly.

The Bragg values are shown against the composition of the Ch_D phase in Fig. 11 to demonstrate the anisotropy of the periodic volume. The values of the periodic volumes of the disklike micelles are of the same order of magnitude.

The micelle parameters of the Ch_D phase with respect to the surfactant content at constant surfactant/cosurfactant ratio (6.65) are summarized in Table 2. With increasing surfactant concentration the micelle volume and the average aggregation number decrease. The same trends were observed for the V_P and $\bar{z}_s$ values in the $C_{16}Me_2EABr$/water/*n*-decanol/taurocholic acid system.

Structural parameters of the Ch_D phase induced by cholesterol, prednisolone and taurocholic acid

The essential structural parameters of the micelles in the Ch_D phase as function of the concentration, c_I of the

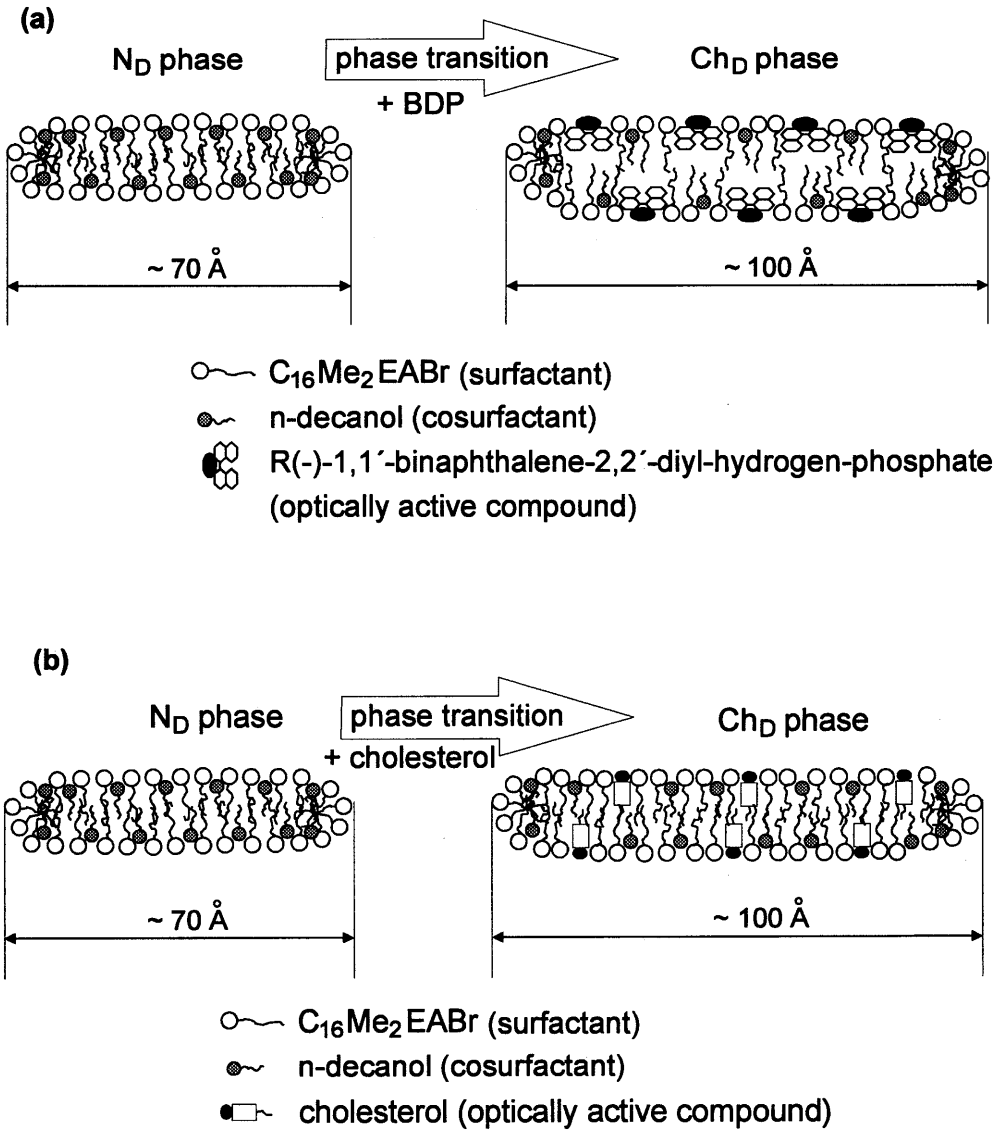

Fig. 8a, b Simplified model to illustrate the solubilization of the optically active compounds BDP and cholesterol in the disklike micelle of the N_D phase forming the Ch_D phase. **a** Solubilization of BDP with axial chirality. **b** Solubilization of cholesterol with center chirality

optically active compounds cholesterol, prednisolone and taurocholic acid are collected in Table 3. The following conclusions can be drawn:

- The periodic volume in $C_{16}Me_2EABr$/water/*n*-decanol/cholesterol increases with increasing c_I. This trend changes in the quaternary systems with prednisolone and taurocholic acid. The periodic volume runs through a maximum.
- The micelle volume (V_M) is strongly dependent on the concentration of the chiral substances. The micelle volume of the systems containing cholesterol increases with rising c_I. On the other hand V_M of the prednisolone- and taurocholic acid containing systems decreases with rising concentrations of the chiral substances.
- The trend of the anisotropy is quite similar to the trend of the periodic volume of the cholesterol, prednisolone and taurocholic acid containing systems.
- The micelle thickness for the systems with cholesterol is independent of c_I and for prednisolone it slightly increases with the prednisolone concentration.
- The micelle diameter of cholesterol rises with increasing c_I. On the other hand, the micelle diameters of the system containing prednisolone run through a maximum.
- The average aggregation numbers, $\bar{z}_A$, for the system containing cholesterol increase systematically with increasing cholesterol concentration. The $\bar{z}_A$ values of the system with prednisolone run through a maximum, similar to the average aggregation numbers of the system containing taurocholic acid.

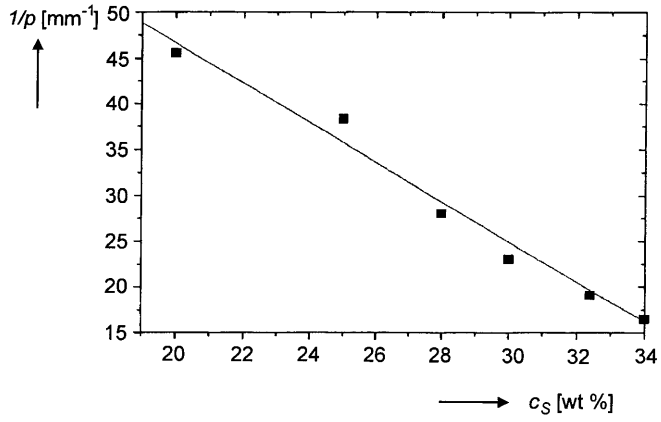

Fig. 9 Reciprocal helix lengths as a function of the $C_{16}Me_2EABr$ concentration, c_S, at constant ratio $C_{16}Me_2EABr$/*n*-decanol = 6.65 and 1.3 wt% BDP at 298 K

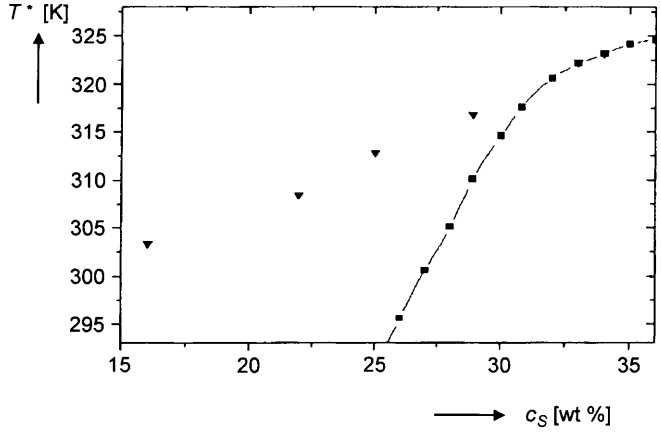

Fig. 10 T^* of the $Ch_D \rightarrow S$ (isotropic phase, ▼) phase transition and the $N_D \rightarrow S$ (■) phase transition as a function of the $C_{16}Me_2EABr$ concentration. Composition of the N_D phase: constant mass ratio $C_{16}Me_2EABr$/*n*-decanol = 6.65. Composition of the Ch_D phase: matrix of N_D phase + 1.3 wt% BDP

– The trend of the average numbers of the solubilized chiral compounds is quite similar. Increasing the concentrations of cholesterol, prednisolone and taurocholic acid increases the $\bar{z}_I$ values in the $C_{16}Me_2EABr$/water/*n*-decanol/chiral component systems.

Comparison of the properties of the Ch_D phase induced by molecules with center chirality and with axial chirality

In previous work [46–48] we discussed the results of X-ray diffraction investigations on the influence of different chiral compounds, such as cholesterol, prednisolone and taurocholic acid, on the induction of the lyotropic

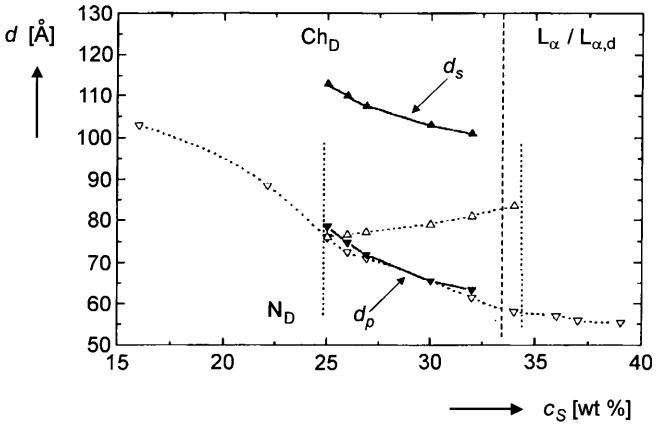

Fig. 11 Anisotropy of the periodic volume in the Ch_D phase as a function of the $C_{16}Me_2EABr$ concentration at 298 K at a constant mass ratio $C_{16}Me_2EABr$/*n*-decanol and 1.3 wt% BDP. N_D, disklike lyotropic nematic phase; L_α, lamellar phase, chains fluid; $L_{\alpha,d}$, lamellar phase with defects

Table 2 Micelle parameters of the induced Ch_D phase as function of the $C_{16}Me_2EABr$ concentration, c_S, at constant mass ratio $C_{16}Me_2EABr$/*n*-decanol = 6.65 and 1.3 wt% BDP

c_s (wt%)	V_P (10^5 Å^3)	V_M (10^5 Å^3)	$A = d_{010}/d_{100}$	$\bar{z}_A$	$\bar{z}_I$
25	7.78	2.35	1.43	314	15.0
27	6.74	2.15	1.52	283	12.2
30	5.52	1.93	1.57	263	10.5
32	5.12	1.76	1.58	240	8.4

cholesteric phase. These optically active molecules are center chiral. In this work we summarized the X-ray results and the results of pitch length measurements in the $C_{16}Me_2EABr/H_2O$/*n*-decanol/BDP quaternary system. BDP is an axial chiral compound. Both types of chiral components form lyotropic cholesteric phases.

In the following part of this article we analyze the differences between the induction properties of molecules with axial and with center chirality during the process of Ch_D-phase formation. The micelle parameters of the Ch_D phase are summarized in Table 4. The data indicate that the solubilization of the optically active component into the micelles of the N_D phase is the most important factor. The solubilization of the chiral dopants changes the micelle anisotropy and the structure of the micelles. This process is independent of the chiral elements in the optically active molecules. Although cholesterol and BDP are very different in chemical constitution, both substances cause a distinct increase in the micelle anisotropy and large differences exist in the HTP values. The HTP value of BDP is 192.3 mm^{-1} mol^{-1} and is essentially lower than for cholesterol (HTP = 357.0 mm^{-1} mol^{-1}). One of the reasons for this difference in the HTP values is probably the molecule lengths of both compounds.

Table 3 Micelle parameters of the induced Ch_D phase with respect to the concentration of the optically active compounds cholesterol, prednisolone and taurocholic acid at 298 K. D_D, micelle thickness; D_M, micelle diameter

c_I (wt%)	V_P (10^5 Å^3)	V_M (10^5 Å^3)	$A = d_{0\,1\,0}/d_{1\,0\,0}$	D_D (Å)	D_M (Å)	$\bar{z}_A$	$\bar{z}_I$
Cholesterol[a]							
0	3.33	1.01	1.14	36	63	139	0
0.27	4.07	1.25	1.19	32	71.5	166	1.7
0.50	4.89	1.50	1.32	30	80	190	3.6
1.00	5.65	1.75	1.40	30	86	220	8.5
1.29	6.11	1.90	1.44	30	90	245	12.5
1.59	6.47	2.04	1.48	30	93	262	16.1
2.1	6.82	2.18	1.54	30	96	270	23.0
Prednisolone[b]							
0	3.64	1.20	1.20	34	64	150	0
0.27	3.85	1.29	1.22	42	70.5	165	1.72
0.5	4.04	1.35	1.26	46	72.5	178	3.3
1.0	4.01	1.36	1.24	47	50	177	6.6
1.4	3.78	1.29	1.18	48	68	167	8.8
2	3.26	1.14	1.07	49	62	144	11
4	2.93	1.05	1.00	51	51	129	14

c_I (wt%)	V_P (10^5 Å^3)	V_M (10^5 Å^3)	$A = d_{0\,1\,0}/d_{1\,0\,0}$	$\bar{z}_A$	$\bar{z}_I$
Taurocholic acid[c]					
0	3.62	1.18	1.26	156	0
0.5	3.82	1.25	1.21	168	2.2
0.9	3.84	1.26	1.14	169	4
1.4	3.80	1.22	1.05	166	5.7
2.0	3.40	1.10	1.02	151	7.7
2.5	3.18	1.03	1	140	9

[a] Composition of the Ch_D phase: 26 wt% $C_{16}Me_2EABr$; 70.06 wt% water; 3.94 wt% *n*-decanol + cholesterol
[b] Composition of the Ch_D phase: 28 wt% $C_{16}Me_2EABr$; 67.7 wt% water; 4.3wt% *n*-decanol + prednisolone
[c] Composition of the Ch_D phase: 28 wt% $C_{16}Me_2EABr$; 67.7 wt% water; 4.3 wt% *n*-decanol + taurocholic acid

Table 4 Comparison of selected micelle parameters of the Ch_D phase of BDP, prednisolone and taurocholic acid at 298 K. HTP, helical twisting power; T^*, temperatures of the $Ch_D \rightarrow S$ transition; c_I, concentration of the inducing substance; $\bar{z}_D$, average aggregation numbers per micelle in the N_D matrix without inducing substance; $\bar{z}_I$, average solubilization numbers of inducing molecules per micelle

Parameter	BDP	Cholesterol	Prednisolone	Taurocholic acid
HTP (mm^{-1} mol^{-1})	192.3	357	425	312.5
$\Delta T^*/\Delta c_I$ (K mol $\%^{-1}$)	92	258	0	–59
$\bar{z}_D$	161	161	160	169
$\bar{z}_A$	298	269	142	149
$\bar{z}_I$	22	23	12	8.2
$A = d_{0\,1\,0}/d_{1\,0\,0}$	1.63	1.54	1.07	1.02

The molecular lengths of $C_{16}Me_2EAB$, *n*-decanol and the optically active compounds cholesterol and prednisolone are derived from molecular models (Fig. 12). The conclusion is that the lengths of the cholesterol, prednisolone and *n*-decanol molecules are of the same order of magnitude. In contrast, BDP and tartaric acid are much shorter. We conclude that only a small part of the BDP and tartaric acid molecules can be incorporated in the micelle. Further information on the chirality transfer from chiral elements on a low-molecular basis to the chiral phase is needed as well as a better understanding of the interactions in the lyotropic cholesteric liquid-crystalline phase. The influence of type, number and position of the hydrophilic groups at the cholestane ring of the center chiral substances determines the solubilization of the inducing dopants in the micelles in the N_D matrix. Without these hydrophilic groups in the optically active substances, for instance by use of cholestane, the liquid-crystalline state was not formed.

Otherwise it is very difficult to find strong correlations between the chemical constitution of chiral substances and their induction properties. The main point for the formation of the Ch_D phase is the capability of the micelles to solubilize the chiral compounds. In this sense the optically active compound acts like a cosurfactant. Dopants with only one polar group in the molecule, like cholesterol and BDP, increase the radius of the disklike micelles. To form the helix a minimum concentration of dopants in the

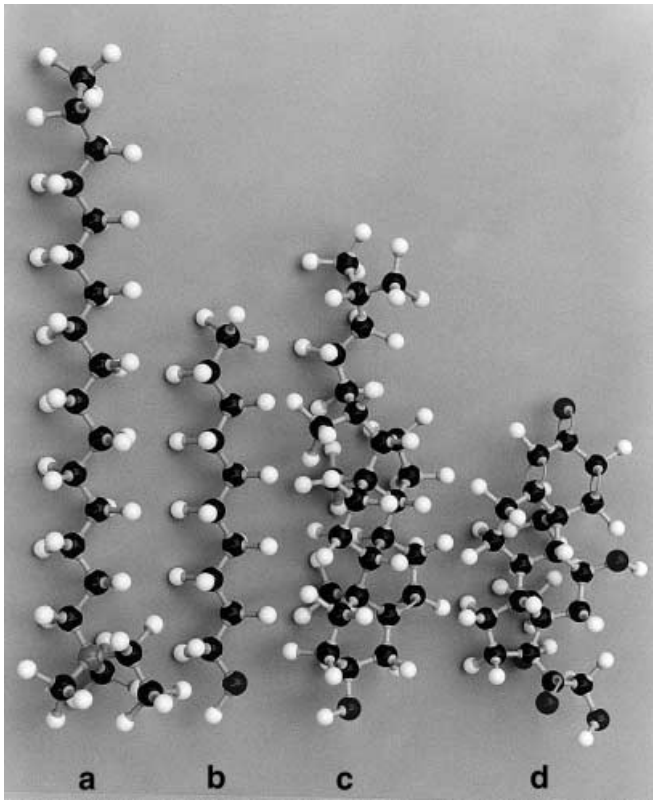

Fig. 12 Molecular models demonstrating the molecule lengths of the compounds which form the micelles in the N_D phase and the Ch_D phase. **a** $C_{16}Me_2EABr$ (surfactant), **b** *n*-decanol (cosurfactant), **c** cholesterol (optically active compound), *d* prednisolone (optically active compound)

micelle is needed, about 1–2 molecules per micelle. Details were described in Refs. [41, 42, 44, 45]. However, the micelles of the Ch_D phase cannot solubilize larger numbers of chiral molecules. In our systems [41, 42, 44, 45] we observed the $Ch_D \rightarrow L_\alpha$ phase transition or the $Ch_D \rightarrow S$ phase transition after reaching the maximum concentration.

A similar phenomenon, i.e. the transition from the lyotropic cholesteric phase into the lamellar phase, was described Hiltrop et al. [70]. The authors studied the temperature dependence of the pitch and approached the lamellar phase by means of several Cs salts of perfluorosurfactant/water mixtures with different mixing ratios, each doped with different optically active compounds. Independent of the chemical constitution of the chiral substances the isotropic to lyotropic cholesteric transition towards the lyotropic cholesteric to lamellar transition at decreasing temperatures increased the pitch. This helix-unwinding behavior at the $Ch_D \rightarrow L_\alpha$ phase transition is comparable to the behavior of thermotropic liquid crystals. This result leads to the conclusion that the $Ch_D \rightarrow L_\alpha$ phase transition is a disorder/order transition of discrete micelles.

Concerning the $Ch_D \rightarrow L_\alpha$ phase transition in our systems, the chiral substances were probably inserted in the micelles in a position where the micelle forms the lowest curvature in their shape. The solubilization of the chiral components increases the anisotropy of the micelles and the temperature of the $Ch_D \rightarrow S$ phase transition. In a similar way the thickness of the bilayers in the disks increased significantly [44–48].

The constancy of the temperature T^* of the $Ch_D \rightarrow S$ phase transition and the decrease in the helix lengths indicate that in the case of prednisolone the helix formation is determined by pairwise interaction between adjacent prednisolone molecules in the helical stack. Thus, anchoring of the polar group in the micelle is very important for inducing properties of the optically active substances.

Conditions of helix formation in lyotropic cholesteric liquid crystals

Our previous studies showed that the solubilization of the chiral molecules in a matrix of a N_D phase induced Ch_D phases. In the case of thermotropic liquid crystals the structural unit is a molecule. The most generally applicable theories which account for nematic and cholesteric phase formation include the assumption of anisotropic dispersion forces or intermolecular potentials [49–52].

The unit of the lyotropic nematic and cholesteric phases of these structures is a mixed micelle, which contains a few hundred individual surfactant and cosurfactant molecules. The geometry of the micelles can be rodlike or disklike. Their characteristic properties are the textures in the polarizing microscope, low-angle X-ray diffraction patterns and spontaneous alignment in a magnetic field.

The long-range orientional order is a consequence of anisotropic forces between large micelles, which may grow in size and even change their symmetry when the chemical structure changes. Thus, the thermotropic cholesteric structure is directly related to the dissymmetry of the basic molecular units. However, aqueous lyotropic cholesteric systems have an intervening level of superstructure. The optically active amphiphilic components are assembled into large micelles, each of which participates in a long-range orientional order of helical form. As the origin of this lyotropic cholesteric state is still not well understood it is not self-evident whether the relationships observed in the thermotropic case between pitch length and mole fraction of the dextro or the levo form are experimentally manifested in the aqueous lyotropic case [53].

To understand these problems we started with systematic investigations. The lyotropic nematic matrix (N_D phase) was prepared in the $C_{16}Me_2EABr/H_2O/$

n-decanol ternary system [41, 43]. To induce the lyotropic cholesteric phase we selected center chiral components as corticoides, androgenes, estrogenes, cardenolides, derivatives of the cholic acid and sterols [41, 42, 44–48]. From the results of our texture observations and by evaluation of the SWAXS measurements of these systems we draw the following conclusions.

(1) Solubilization properties of the micelles in the N_D phase:

- The formation of micelles in the N_D phase and the Ch_D phase takes place under dynamic conditions. First of all we have to take into the account the thermodynamic equilibrium between "monomers" (single molecules) and micelles. The micelles have quasi the properties of fluids, which are able to solubilize cosurfactants and chiral components. We have to consider that a complicated four-component system is formed with "mixed micelles" containing surfactant, cosurfactant and optically active compounds.
- Helix formation starts with about 1–2 chiral molecules per micelle in the N_D phase (see Table 3). The chiral substances act as cosurfactants.
- The cosurfactant and the optically active molecules are of about the same length (Fig. 12). Probably, the chiral compounds are incorporated in a position parallel to the hydrophobic part in the bilayer of the disklike micelles.
- The size and the geometry of the micelles change during the solubilization of the chiral components into the micelles of the N_D phase (Table 3).

(2) Interaction between the micelles in the Ch_D phase:

- In the first step during helix formation the chemical constitution and geometry of the chiral compound is responsible for the mechanism of solubilization in the micelle. For instance, cholesterol, containing only one polar group (HO group), is flexible in the apolar part. So the insertion into the micelles can occur without steric difficulties. In contrast, prednisolone contains various polar groups (C = O and HO groups), whereas the axial chiral BDP molecule is very rigid.
- Hydrogen bonds are also very important. For instance, prednisolone forms hydrogen bridges between adjacent molecules in the helical stack. The hydrogen bridges between two neighboring micelles act like a "hinge joint" and bring the two micelles in a fixed position. We assume that the chiral molecules are "swimming" in the micelles, i.e. their position is variable, and so we propose a simple model of how the helix is formed (Fig. 13).

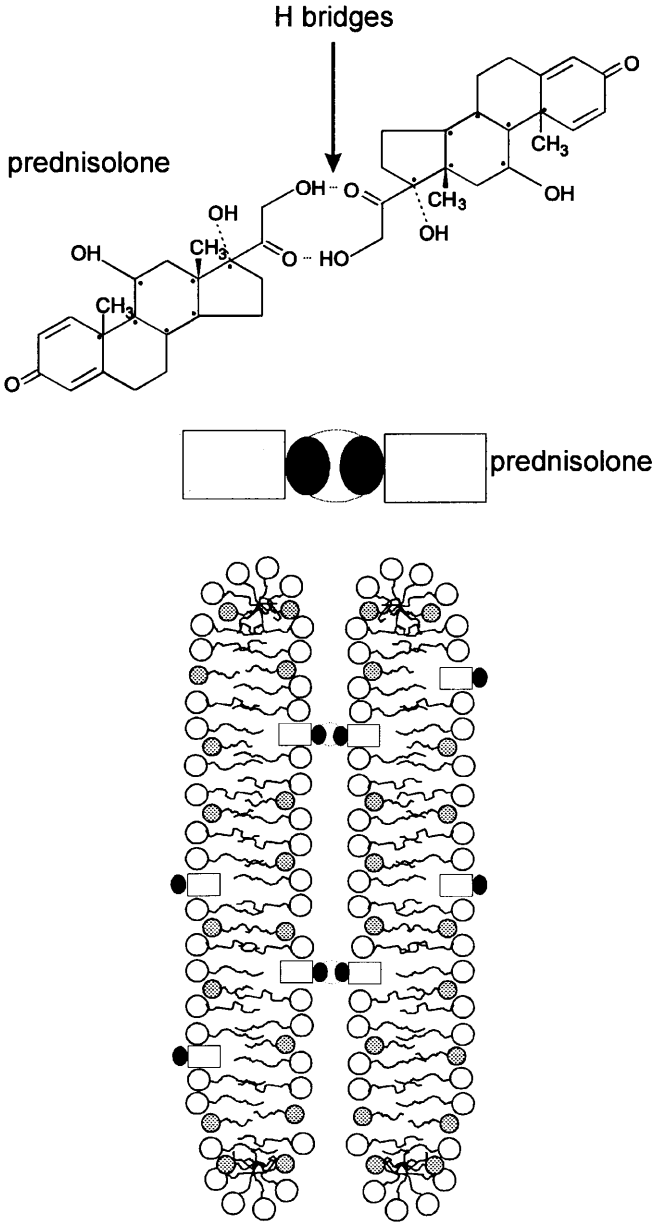

Fig. 13 Simplified model demonstrating the interaction between two prednisolone molecules arranged in two micelles of the helical stack forming the hydrogen bridges

- We assume that, on average, 3–20 chiral molecules are solubilized in a micelle. This number depends on the concentration of the chiral component and on the surfactant/cosurfactant ratio. Probably, the distribution of the chiral components in the micelles is not homogeneous and the components are in a partially "demixed state" in the micelle. The chiral molecules are located at sites where the micelle has the smallest curvature. The chiral dopants are then able to form the "hinge joint" for the formation of hydrogen bridges between two neighboring micelles (Fig. 13).

(3) Changes in the micelle curvature and induction of the phase transition to the lamellar or isotropic phase:

- The incorporation of the dopants into the micelles changes the curvature at the water/micelle interface because the optically active compound acts like a cosurfactant and lowers the interface tension. The optically active compounds reduce the mean head group area and the interface curvature changes. A spherical micelle may transform into a cylindrical one, a rod turns into a lamella. On increasing the concentration of the surfactant the shape of the micelles must also change because of the repulsion between the aggregates. At a fixed concentration of the surfactant, spheres have the smallest intermicellar distances compared to rods or disks. Hence, to minimize the free energy, a lyotropic system can change from globular to rodlike or disklike micelles.
- This change of the curvature of the micelles in the Ch_D phase correlates with phase transitions. The phase transition occurs at a characteristic concentration, c_{max}, which depends on the chemical constitution of the chiral molecule and the composition of the N_D phase. We observed the $Ch_D \rightarrow L_\alpha$ phase transition (see texture of the lamellar phase, Fig. 2d) as well as the $Ch_D \rightarrow S$ transition [44, 45].
- The incorporation of the chiral substances into the micelles leads to a change in the micelle geometry and anisotropy. The average aggregation number of the micelles also changes (Table 3). Furthermore, the thickness of the bilayer of the disklike micelles increases significantly. This means that pairwise interactions between the adjacent chiral molecules in the helical stack are not dominant.
- We observed constant T^* values for the $Ch_D \rightarrow S$ phase transition and a decrease in the micelle anisotropy and of the helix length with rising prednisolone concentration [48].

(4) Mechanism of helix formation:

- Owing to the incorporation of the chiral substances into the micelles, the chirality in the micelles probably changes. Details of this mechanism are not quite clear. We observe helix formation by center chiral compounds as well as by axial chiral dopants.
- The first step during the helix formation, as mentioned already, is the solubilization of the dopants into the micelles. The interaction between the optically active molecules results in the formation of hydrogen bridges between the adjacent optically active molecules in the helical stack (Fig. 13).
- For helix formation a minimum concentration, c_{min}, of the optically active component is needed [41–48]. Molecules with center chirality as well as molecules with axial chirality can build helices.
- The HTP values are dependent on the chemical constitution of the inducing molecules and on the composition of the N_D phase (Tables 1–4).
- During helix formation the number of micelles per helix length changes as a function of the concentration of the chiral molecules.
- The twisting power of our compounds [41, 42, 44–48] varies by nearly 2 orders of magnitude. The number of active carbon atoms in the center chiral compounds is between 2 (tartaric acid) and 23 (digitoxin) [41–48]; however, this fact does not explain the low twisting effect of tartaric acid. The twisting power depends significantly on the position of the optically active compound in or at the micelles.

Conclusions

In our systematic investigations [41–48] on the mechanism of helix formation in a matrix of N_D phases we described the essential experimental conditions which are necessary for building lyotropic cholesteric phases by adding chiral compounds. The application of center chiral as well as axial chiral substances leads to the $N_D \rightarrow Ch_D$ phase transition in the surfactant/cosurfactant/water ternary system of the lyotropic nematic matrix. Our texture observations and SWAXS measurements were very good tools for identifying the phases, for measuring the helix lengths and for deriving structural parameters of the micelle size and micelle geometry in the N_D phase and in the Ch_D phase.

For the formation of the Ch_D phase, the solubilization properties of the N_D phase matrix is the important factor. The solubilization capacity of the micelles in the N_D phase is strongly dependent on the composition of the N_D phase and on the chemical constitution of the chiral compound. Helix formation starts in the N_D phase when about 1–2 chiral molecules are present in the micelle. The chiral substances act like cosurfactants. The incorporation of the chiral substances in the micelles changes the curvature of the micelles. The chiral compounds are located in sites where the micelles have the smallest curvature. The bonds between the disks in the helix are probably hydrogen bridges between adjacent chiral molecules. The hydrogen bridges between two neighboring micelles act like hinge joints and hold the two micelles in a fixed position.

A further interesting aspect is the induction of the phase transition from the Ch_D phase in the L_α phase or in the isotropic phase after reaching c_{max}. The chiral substance reduces the mean head group area and changes the interface curvature, for example, a disk turns into a lamella. Owing to the insertion of the chiral substances into the micelles, the chirality in the micelles

probably changes; however, these problems are not quite clear. A further outstanding question is the role of optically active carbon atoms during helix formation.

Acknowledgements It is a pleasure to thank Carsten Görgens for his help with the SWAXS measurements. Financial support of the Deutsche Forschungsgemeinschaft (Germany) is acknowleged.

References

1. Zugenmaier P (1997) In: Kuczynski W (ed) Self-organization in chiral liquid crystals. Scientific Publishers OWN, Poznan, Poland, p 97–117
2. Hashimoto T, Ouaba N, Ebisu S, Kawai H (1981) Polym J Tokyo 13:897
3. Ernst B, Navard P, Hashimoto T, Takeba T (1990) Macromolecules 23:1370
4. Forrest BJ, Reeves LW (1981) Chem Rev 81:1–14
5. Onogi Y, Tokumitsu K (1990) Chem Express 5:201
6. Onogi Y, Okubo T (1992) Liq Cryst 12:815
7. Cai B, Zhang G, Wu F, Gao H (1992) Gaofenzi Cailiao Kexue Yu Gouy Cheng 8:71
8. Guo JY, Gray DG (1989) Macromolecules 22:2082
9. Harkness BR, Gray DG (1989) Polym Prepr Am Chem Soc Div Polym Chem 31:644
10. Harkness BR, Gray DG (1990) Liq Cryst 8:237
11. Budgele D, Gray DG in: Polymer Fiber Sci: Recent Adv., ed. Formes, Raymon:145
12. Zugenmaier P (1990) Papier 43:658
13. Siekmeyer M, Zugenmaier P (1990) Cellulose:347
14. Bonazzi S, Capobianco M, DeMorais MM, Gorbesi A, Gottarelli GM, Marianni P, Ponzi B (1991) J Am Chem Soc 113:5809
15. Spada GP, Carcuro A, Colonna FP, Gorbesi A, Gottarelli GM (1988) Liq Cryst 3:651
16. Tracey AS, Diehl P (1975) FEBS Letters 59:131
17. Figueiredo Neto AM, Galerne Y, Liebert L (1985) J Phys Chem 89:3939
18. Forrest BJ, Reeves LW, Vist M (1984) Mol Cryst Liq Cryst 113:37
19. Tracey AS, Radley K (1984) J Phys Chem 88:6044
20. Alcantara MR, Vanin JA (1984) Mol Cryst Liq Cryst 102:7
21. Melnik G, Saupe A (1987) Mol Cryst Liq Cryst 145:95
22. Kroin T, Figueiredo Neto AM, Liebert L, Galerne C (1989) Phys Rev A Gen Phys 40:4667
23. Alcantara MR, de Melo MV, Paoli VR, Vanin JA (1993) J Colloid Interface Sci 93:560
24. Figueiredo Neto AM, Helene MEM (1987) J Phys Chem 91:1466
25. Helene MEM, Figueiredo Neto AM (1988) Mol Cryst Liq Cryst 127:1623
26. Lee H, Labes MM (1978) Mol Cryst Liq Cryst 44:227
27. Goldfarbs D, Mosley ME, Labes MM, Luz Z (1982) Mol Cryst Liq Cryst 89:119
28. Lee H, Labes MM (1982) Mol Cryst Liq Cryst 84:137
29. Lee H, Labes MM (1983) Mol Cryst Liq Cryst 82:335
30. Lee H, Labes MM (1984) Mol Cryst Liq Cryst 108:125
31. DoAido M, Alcantara MR (1991) Mol Cryst Liq Cryst 195:45
32. Forrest BJ, Mattai J (1984) Chem Phys Lipids 35:1
33. Alcantara MR, Vanin JA (1986) Quimica Nova 2:185
34. Forrest BJ, Reeves LW, Vist MJ (1981) J Am Chem Soc 103:690
35. Tracey AS, Radley K (1990) Langmuir 6:1221
36. Alcantara MR, de Melo MV, Paoli VR, Vanin JA (1983) Mol Cryst Liq Cryst 90:335
37. Krämer U (1990) Thesis. University of Bayreuth, Germany
38. Valente Lopes MC, Figueiredo Neto AM (1988) Phys Rev A 38:1101
39. Acimis M, Reeves LW (1980) Can J Chem 58:1533
40. Radley K, Saupe A (1978) Mol Phys 35:1405
41. Bartusch G, Dörfler HD, Hoffmann H (1992) Progr Colloid Polym Sci 89:307
42. Dörfler HD, Friedrich G, Swaboda C (1995) Tenside Surfactants Deters 32:244
43. Friedrich G, Dörfler HD (1995) Tenside Surfactants Deters 32:252
44. Dörfler HD, Swaboda C (1998) Tenside Surfactants Deters 35:18
45. Dörfler HD, Swaboda C (1998) Tenside Surfactants Deters 35:126
46. Dörfler HD, Görgens C (1999) Tenside Surfactants Deters (in press)
47. Dörfler HD, Görgens C (1999) Tenside Surfactants Deters (in press)
48. Dörfler HD, Görgens C (1999) Tenside Surfactants Deters (in press)
49. (a) Maier W, Saupe A (1958) Z Naturforsch 139:564; (b) Maier W, Saupe A (1959) Z Naturforsch 149:882; (c) Maier W, Saupe A (1960) Z Naturforsch 159:287
50. Luckhurst GR (1979) In: Luckhurst GR, Gray GW (eds) The molecular physics of liquid crystals. Academic, New York, p 85
51. DeGennes PG (1969) Mol Cryst Liq Cryst 7:325
52. Schroder H (1979) In: Luckhurst GR, Gray GW (eds) The molecular physics of liquid crystals. Academic, New York, p 121
53. (a) Bak CS, Labes MM (1975) J Chem Phys 62:3066; (b) Bak CS, Labes MM (1975) J Chem Phys 63:805
54. Finkelmann H, Stegemeyer H (1974) Ber Bunsenges Phys Chem 78:869
55. Stegemeyer H (1974) Ber Bunsenges Phys Chem 78:860
56. Voss J, Sackmann E (1973) Z Naturforsch A Phys Sci 28:1496
57. Pollmann P, Stegemeyer H (1974) Ber Bunsenges Phys Chem 78:843
58. Lawson KD, Flautt TJ (1967) J Am Chem Soc 89:5490
59. Rosevear FB (1968) J Soc Cosmet Chem 19:581
60. Boden N (1994) In: Gelbart WM, Ben-Shaul A, Roux D (eds) Micelles, membranes, microemulsions, and monolayers. Springer, Berlin Heidelberg New York, p 153
61. Ben-Shaul A, Gelbart WM (1994) In: Gelbart WM, Ben-Shaul A, Roux D (eds) Micelles, membranes, microemulsions, and monolayers. Springer, Berlin Heidelberg New York, p 1
62. Yu LJ, Saupe A (1980) J Am Chem Soc 102:4879
63. Amaral LQdo, Freire Pimentel C, Tavares MR, Vanin JA (1979) J Chem Phys 71:2940
64. Amaral LQdo, Tavares MR (1980) Mol Cryst Liq Cryst Lett 56:203
65. Forrest BJ, Reeves LW (1981) Chem Rev 81:1
66. Hendrikx Y, Charvolin J (1981) J Phys 42:1427
67. Adams J, Haas W (1975) Mol Cryst Liq Cryst 30:1
68. Goossens WJA (1971) Mol Cryst Liq Cryst 12:237
69. Dörfler HD, Görgens C (1999) Tenside Surfactants Deters (in press)
70. Hiltrop K, Figgenmeier E, Pape M, Partyka J (1997) In: Kuczynski W (ed) Self-organization in chiral liquid crystals. Scientific Publishers OWN, Poznan, Poland, p 35
71. Frank FC (1958) Discuss Faraday Soc 25:19
72. Oseen CW (1925) Ark Mat Astron Fys A19:1